Int. J. Electrochem. Sci., 17 **(2022)** Article Number: 22119, doi: 10.20964/2022.11.12

International Journal of
ELECTROCHEMICAL
SCIENCE
www.electrochemsci.org

Simulation and optimization of an Electrocoagulation integrated device

Liu Yang[1,2], Wu MingRui[1,2], Zhang Jie[3], Zhang Xue[1,2], Li ZhiHui[1,2], Jiang WenMing[1,2,4,]*

[1] College of Pipeline and Civil Engineering, China University of Petroleum (East China)
[2] Shandong Provincial Key Laboratory of Oilfield Produced Water Treatment and Environmental Pollution Control (Sinopec Petroleum Engineering Corporation), Shandong Provincial Key Laboratory of Oil & Gas Storage and Transportation Safety
[3] China Construction Second Engineering Bureau Co. Ltd
[4] Shandong Provincial Key Laboratory of Oilfield Produced Water Treatment and Environmental Pollution Control (Sinopec Petroleum Engineering Corporation), Dongying 257061, China;
[*]E-mail: jiangwenming@upc.edu.cn

Received: 28 June 2022 / *Accepted:* 29 August 2022 / *Published:* 10 October 2022

Electrocoagulation as an environment-friendly technology has been proven to remove pollutants with high efficiency. However, the development and optimization of Electrocoagulation integrated devices hinder its industrial application. This paper aims to design an Electrocoagulation integrated device with high efficiency. Because the velocity distribution of the sedimentation tank was found to significantly affect the treatment efficiency of the integrated device, emphasis would be placed on structural optimization of sedimentation tank. Firstly, a model was established to study the influence of inlet flow and baffle clearance on flow field distribution in sedimentation tank. Secondly, the integrated device was machined by using the parameters obtained from the simulation and tested. The final oil and turbidity removal rate were 90.49% and 85.27% respectively, and there was still room for optimization. Finally, three programmes (changing the position of the upper and lower gaps of the baffle, changing the ratio of the baffle clearance to the corridor width, and changing the corridor width) were carried out. The results showed that optimized flow field was more conducive to the formation of flocs.

Keywords: Oily wastewater; Electrocoagulation; Flow field simulation; Optimization

1. INTRODUCTION

Since the internal combustion engine was invented, exploitation of oil and other resources have been accelerated. Oily wastewater generated during oil extraction was discharged illegally, causing pollution and damage to the environment[1-3]. The composition of oily wastewater is complex[4], and it has the characteristics of small oil-water density difference, high COD and BOD value, and insoluble in water. Besides, the degree of emulsification is high, and it is difficult to decompose naturally[5]. All

of these lead to the difficulties of oil-water separation. Concurrently, with the increasing awareness of environmental protection, the issue of oily wastewater treatment has also received more and more attention. Therefore, an efficient oily sewage treatment method is urgently needed. Chemical coagulation[6], adsorption[7], electroflotation[8], and biodegradation technologies[9] emerge as the times require. However, there are also many problems, including low oil-water separation efficiency, poor stability, small capacity, and secondary pollution[10, 11]. As a sewage treatment technology, Electrocoagulation (EC) technology provides a better alternative because of its high efficiency, simple operation, and environmental protection[12]. Compare to chemical coagulation, this technology does not require the addition of chemicals. Moreover, the removal rate of pollutants is higher than that of chemical coagulation, and the sludge generated is also less than chemical coagulation[13]. Szpyrkowicz compared the removal efficiency of EC and electroflotation under the same conditions and found that EC is more conducive to the treatment of oily sewage[14]. Sadik used EC to treat reactive dye wastewater from textile mills. The results showed that the EC process could achieve the highest wastewater removal rate[15].

EC uses sacrificial metals such as iron and aluminum as anodes. Under the action of current, the anode is dissolved to produce Al and Fe cations. After a series of reaction processes, it develops into various hydroxyl complexes, polynuclear hydroxyl complexes, and even hydroxides. These flocs can adsorb oil particles in oily wastewater. Furthermore, the cathode reduction action produces hydrogen, which lifts the oil away from the water[16, 17]. A comparison between aluminum flocs and iron flocs has been made. The result shows that aluminum flocs have a better adhesion capacity than iron flocs due to the large number of hydrogen bubbles in aluminum flocs. Therefore, the aluminum electrode has a higher efficiency[18]. Then take the aluminum electrode as an example. The electrochemical reaction can be seen in Eq 1 to Eq 3.

At the anode, the aluminum metal is oxidized to aluminum cations[19]

$$Al\ (s) \rightarrow Al^{3+}\ (aq) + 3e^- \qquad (Eq1)$$

Aluminum ions undergo a series of reactions, shown in Eq2, to form hydroxide flocs with surface hydroxides. Due to its large specific surface area, impurities in the water can be absorbed by bridging, netting, and sweeping.

$$2Al + 6H_2O \rightarrow 2Al\ (OH)_3 + 3H_2 \qquad (Eq2)$$

Meanwhile, hydrogen evolution occurs at the cathode, generating a large number of hydrogen bubbles. The reaction is expressed below.

$$2H_2O + 2e^- \rightarrow H_2\uparrow + 2OH^- \qquad (Eq3)$$

At present, the research on EC technology mostly focuses on small devices[14, 15, 18, 19]. Although the experimental operation of the small device is simple and easy to explore the EC mechanism, its small size makes it unsuitable for industrial applications. Therefore, based on previous research on device integration in our group[20], a large-scale integrated EC device was designed in this paper. The sewage storage tank, EC reaction area, sedimentation tank and pumps were combined together which were dispersed previously. It can be easily transported without disassembly. When arriving at the designated place, the device can be used after connect it to the power supply.

The research on water treatment devices using EC usually includes experimental research and computational fluid dynamics (CFD) simulation. Some researchers have studied the effect of EC

technology in the treatment of different pollutants through experiments. Alam[21] used EC to treat acid mine wastewater. The results showed that EC could not only restore the pH value of wastewater to neutral but also remove 99.89% Fe in wastewater. Rahman[22] used EC to treat tropical brackish peat water. He found that while maximum reduction efficiency at 94.09% of color, 89.91% of total suspended solids, 63.19% of pH, 78.93% of electrical conductivity, 92.71% of chemical oxygen demand, 80% of salinity, and 86.04% of turbidity, the treatment cost per cubic meter of sewage was the only US $0.03. In addition, some researchers have combined EC technology with other water treatment methods to further improve the efficiency of sewage treatment and types of processable pollutants. Zhang[23] proposed a new concept that combined in-situ EC with Ni-functionalized conductive membranes for efficient oil/water separation. Conductive Ni@PVA membrane and Al mesh were used as cathode and anode respectively, and a certain current density was applied to form an in-situ EC process. Finally, the oil removal rate could reach 99.4%. Özyonar[24] has studied the treatment of domestic sewage and found that although EC technology could effectively remove chemical oxygen demand（COD）, Escherichia coli, phosphate-phosphorus, nitrite-nitrogen, nitrate-nitrogen, and turbidity in sewage, it could not remove ammonium-nitrogen. Therefore, after the combination of electrocoagulation and electrooxidation, the removal rates of COD, ammonium-nitrogen, and Escherichia coli can reach 95.4%, 89.4%, and 99.99% respectively. In conclusion, most of the experiments focus on the treatment effect of EC reactors but neglected the research on the sedimentation area and the design of integrated sewage treatment devices using EC. According to the previous research of our research group[18, 19, 25], it was found that the structure of the sedimentation area has a significant influence on the final treatment effect of the integrated device when EC reactor is used as the pretreatment. Therefore, it is necessary to use CFD technology to assist research.

CFD simulation with characteristics of accurate results and time-saving is widely used by many researchers. Wang[26] studied the flow field in an EC reactor by CFD and optimized it with experiment, which greatly improved the treatment efficiency of the device. Di[27] used CFD to study and optimize the influence of the plate arrangement on the flow pattern in EC reactor. The results showed that the mass transfer of EC reactor was strengthened and the treatment efficiency was improved. Martinez-Delgadillo[28] evaluated a rotating ring electrode reactor using CFD and studied the influence of hydrodynamic parameters on the treatment process. Höhne[29] studied the degassing process in the EC reaction process using CFD. The results showed that the degassing cycle could be optimized, which was more conducive to the formation and migration of flocs and improved the reaction efficiency of the device. Many researchers had used CFD to study the electroflocculation device. But most of the research only focus on the optimization and research of the EC reactor and did not involve the study of other processing units, such as sedimentation tanks. In actual use, the water treatment plant is a whole. So, it is necessary to test the overall performance of the water treatment plant to guide the design of the experimental device.

In this paper, an integrated device using EC was designed. Without considering the electric field, this integrated device was tested and optimized by numerical simulation and experiment. Because sedimentation tank has a great influence on the treatment efficiency of plants and the relevant research is slightly insufficient, emphasis was placed on the influence of the inflow rate and baffle clearances to the sedimentation tank. And based on the experiment, three optimization schemes were proposed:

changing the position of the upper and lower gaps of the baffle, changing the ratio of the baffle clearance to the corridor width, and changing the corridor width. The flow field distribution after optimization in the device was ideal, which conformed to the growth law of flocs.

2. EXPERIMENTAL EQUIPMENT AND MODEL ESTABLISHMENT

2.1 Experimental device and process

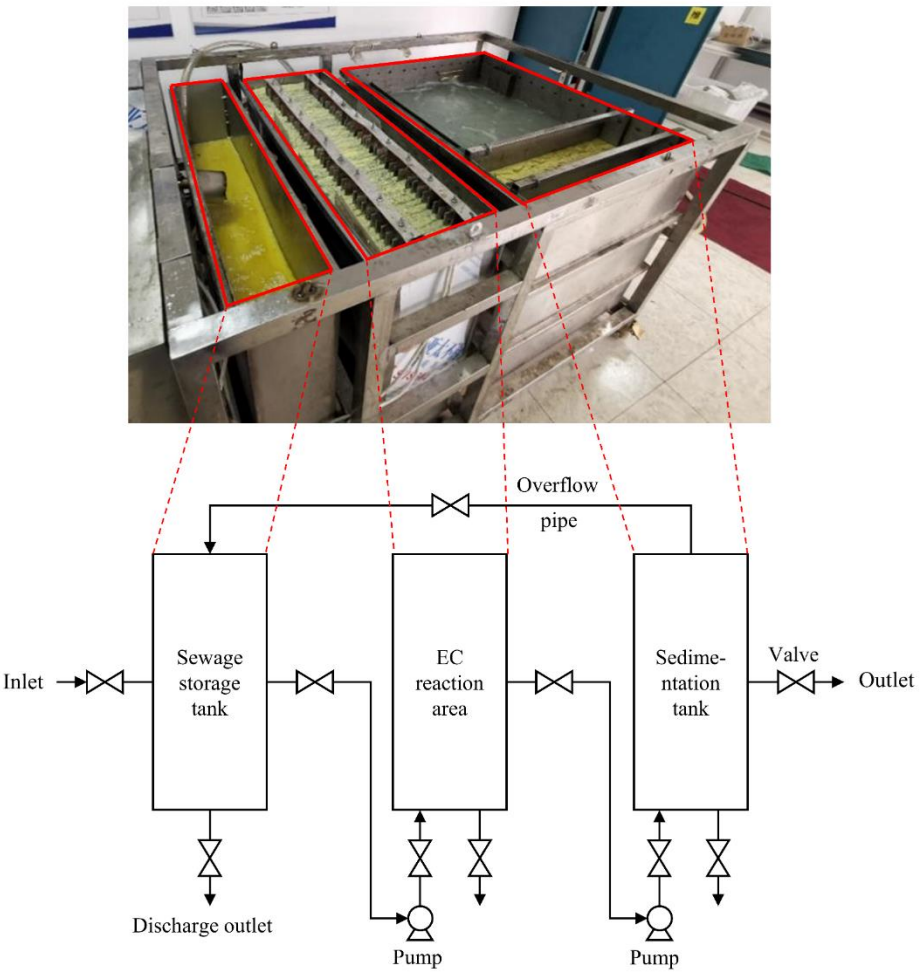

Figure 1. Integrated EC device and schematic diagram

The apparatus used in this experiment, shown in Figure 1, is a purifying integrated device for oily sewage using EC. The equipment consists of a sewage storage tank, an EC reaction area, and a sedimentation tank. Sewage enters the water storage area from the inlet of the water storage area, and is pumped to the EC reaction area through a connecting pipe. Reacted water is pumped to the sedimentation tank after reaction. In the sedimentation tank, there are inclined plate sedimentation device, pressurized air flotation device, foam trapping device, and water outlet. Furthermore, the upper portion of the sedimentation tank is provided with an overflow opening, and connected to the sewage storage area by the overflow pipe.

2.2 Modeling and simulation

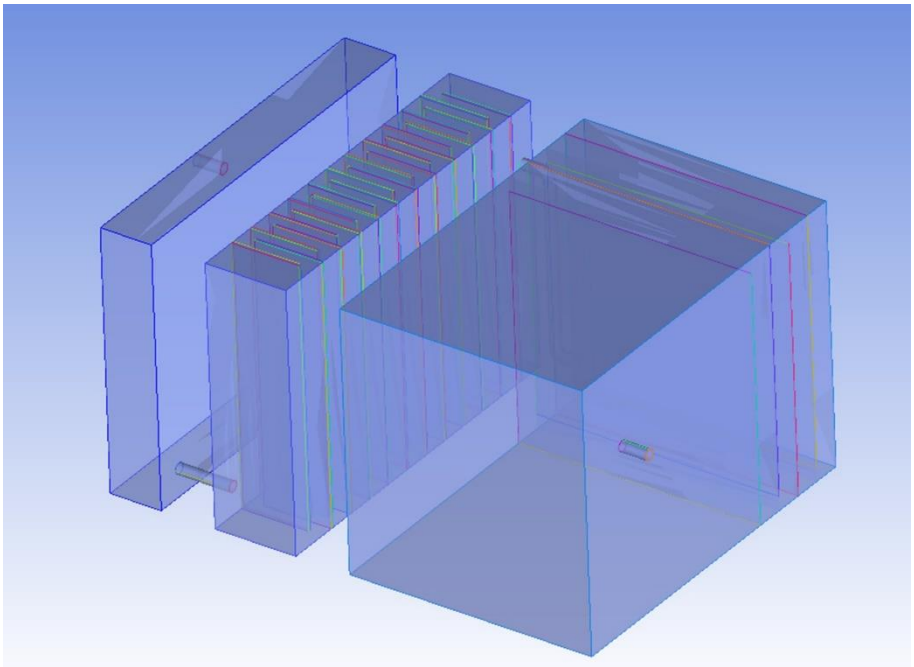

Figure 2. Simplified geometric model

In this paper, ICEM CFD was used to model building and meshing. As shown in Figure 2, the simplified experimental setup consists of a reaction area, a sewage storage tank, and a sedimentation tank. In this simulation, considering the convenience of geometric modeling and grid division, the four cylindrical electrodes are simplified into a rectangular parallelepiped electrode reaction area. The sewage flow method is the same as the original device. Inside the settling tank, there are four baffles with different heights from the top and bottom.

For its fast calculation speed and accuracy, Fluent was chosen as the simulation software. In this simulation, relevant parameters in Fluent are set as follows.

Table 1. Parameter setting in Fluent

Solver type	Pressure-Based
Gravity acceleration	-9.81 m s^{-2}
Model	standard k-ε
Initial residual	10^{-4}
Inlet	velocity-inlet

To explore the influence of the number of grids on the flow field simulation, four models with different numbers of grids were selected. The number of grids is 246133, 446496, 635204, and 852717. The velocity at the centerline of the outlet is selected as the basis. The verification results are shown below.

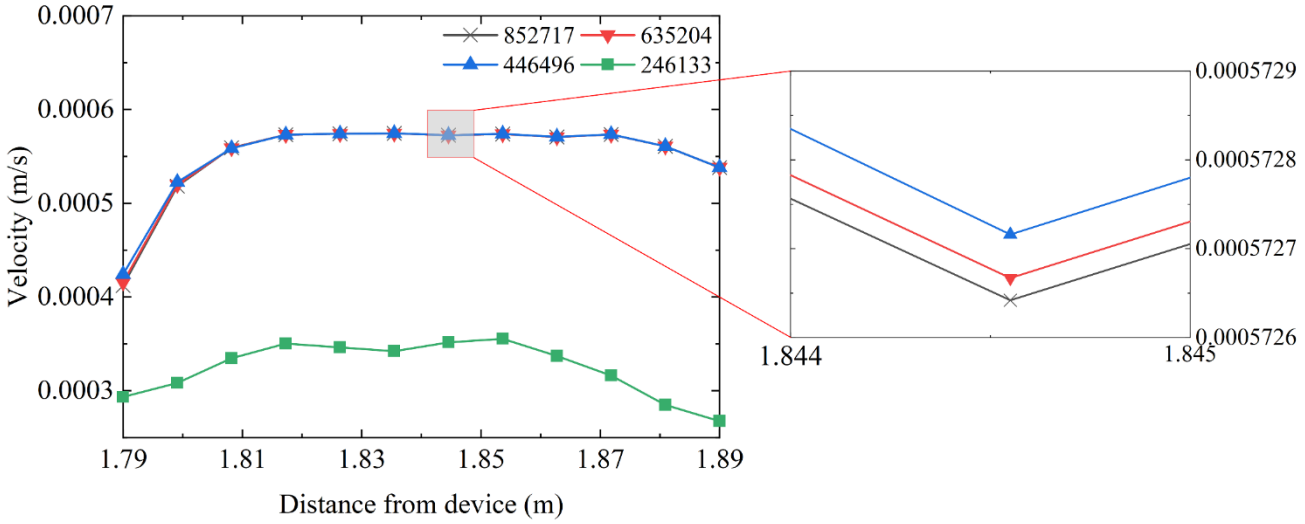

Figure 3. Grid Number Verification

It can be seen from Figure 3 that when the grid number was 246133, the velocity of the outlet pipe was much lower than that of the other three groups. And the fluctuation amplitude was larger than the other three groups. The effect of the simulation was poor at this time. However, when the grid number reached 446496 or above, the interference of the model to the numerical results was small. And there was little difference in the velocity distribution. It can be considered that 446496 has met the requirements of flow field analysis. Therefore, the simulation would be based on the grid number 446496.

3. RESEARCH ON INFLUENCING FACTORS OF FLOW FIELD IN INTEGRATED OILY SEWAGE TREATMENT DEVICE

3.1 Effect of the inflow on sedimentation tank

The flow field distribution in oily sewage treating device using EC has a great influence on the purification process[30, 31]. And the reasonable distribution of the flow field can make the EC process more efficient. Without considering the effect of electrochemistry, six groups of flow were simulated by FLUENT: 0.5 m^3 h^{-1}, 1 m^3 h^{-1}, 2 m^3 h^{-1}, 3 m^3 h^{-1}, 4 m^3 h^{-1}, and 5 m^3 h^{-1}. By observing the flow field distribution at different flows, the regular pattern of flow on flow field would be explored.

Taking the gap between the upper and lower baffle 5cm as an example, the research was carried out. According to the streamline diagram shown in Figure 4, when the inlet flow was 0.5 m^3 h^{-1}, the streamline after passing through the baffle was evenly distributed. And regions with different velocity gradients would be formed between the wall and the baffle.

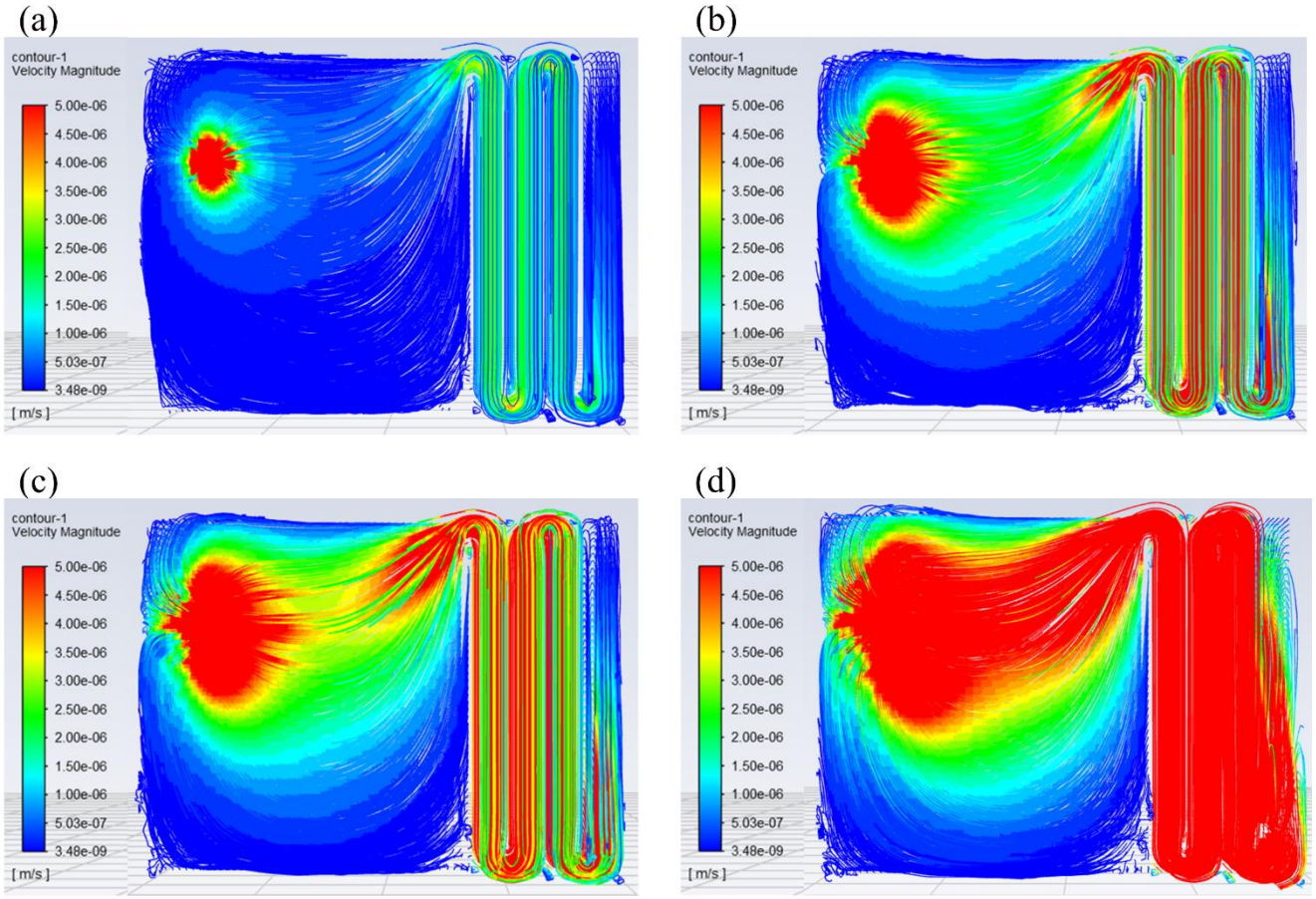

Figure 4. Streamline of sedimentation tank with clearance of 5 cm and flow rate of (a) Q = 0.5 m^3 h^{-1}, (b) Q = 2 m^3 h^{-1}, (c) Q = 3 m^3 h^{-1}, (d) Q = 5 m^3 h^{-1}

Among them, the low-velocity gradient occupied a large area. As the inflow increased, the number of velocity gradients increased, and the area of each velocity gradient became more uniform. When the inflow increased to 2 m^3 h^{-1}, the number of velocity gradients no longer increased. When the flow rate was further increased, the velocity gradient tended to decrease, and the area with higher flow velocity became larger. At present, it might have a violent impact on the surrounding fluid, resulting in the breakage of flocs[32].

According to the velocity nephogram shown in Figure 5, a jet would be formed after the fluid passed through baffles. The larger the inflow, the larger the jet area. The velocity of fluid passing through the baffle did not decrease immediately, but decayed gradually and tended to be stable. When the inflow was 0.5 m^3 h^{-1}, the velocity after passing through the baffle was small and had little disturbance to surroundings. While the inflow increased to 5 m^3 h^{-1}, the velocity passing through the baffles increased significantly. Although the disturbance caused becomes larger, it might lead to the breakage of flocs[30].

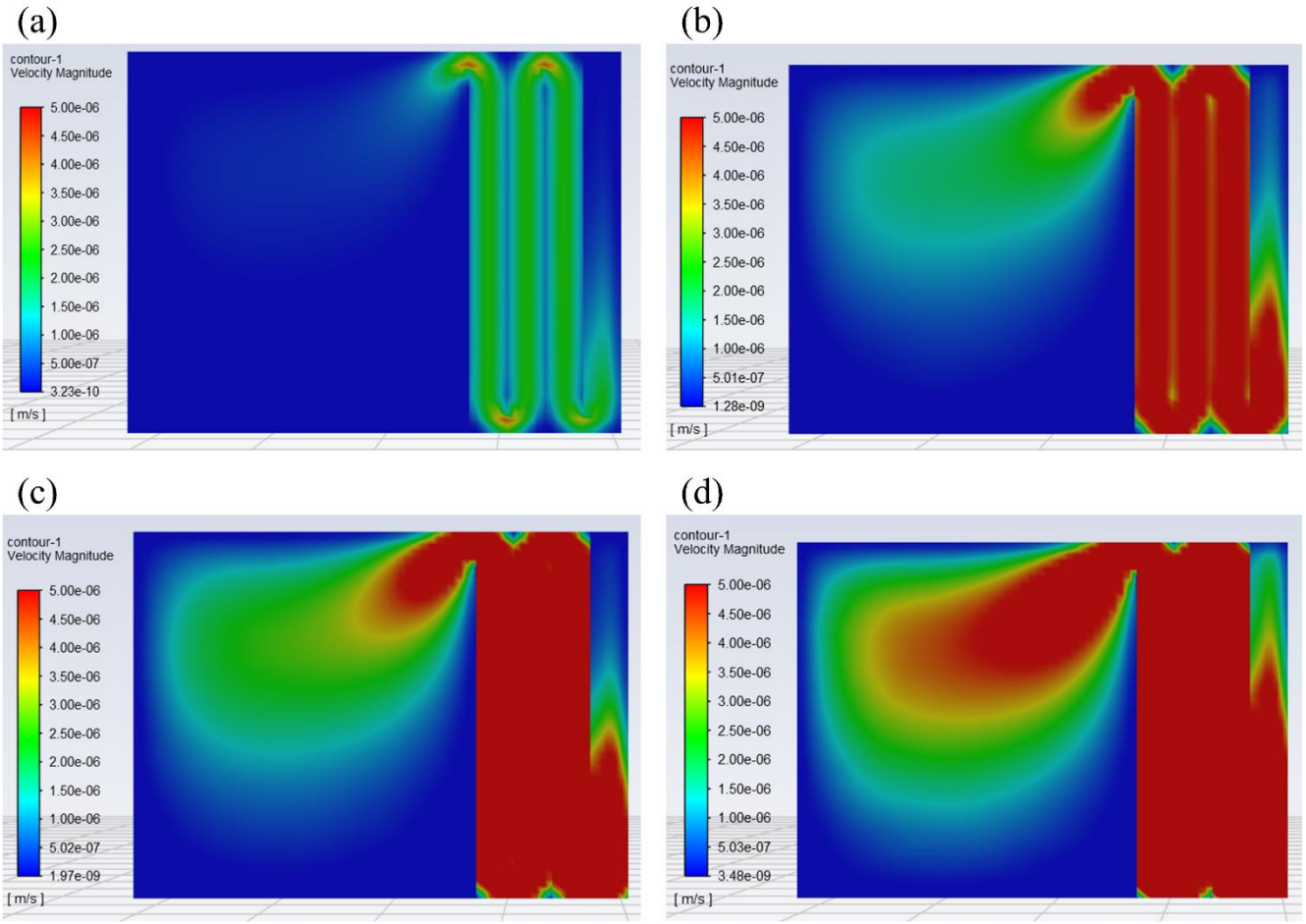

Figure 5. Nephogram of sedimentation tank with clearance of 5 cm and flow rate of (a) Q = 0.5 m^3 h^{-1}, (b) Q = 2 m^3 h^{-1}, (c) Q = 3 m^3 h^{-1}, (d) Q = 5 m^3 h^{-1}

According to the research of Zhou[33], a multi velocity gradient could create a more suitable environment for efficient particle collision and floc growth. It is more beneficial for the formation of flocs with a larger size, density, and better settleability. The reason is that at the initial stage of EC, the particles were small and a high flow rate was required, which could increase the collision probability and enhance mass transfer. After the flocs became larger in the later stage, the shear resistance capacity decreased, and a lower flow rate was required to avoid breaking. Therefore, in practice, the speed gradient and the growth of particles should be considered comprehensively, and the inflow rate should be selected reasonably to create a flow field more conducive to the growth of particles.

3.2 Effect of different baffle clearance

For the sake of achieving a better baffling effect, there were 4 baffles in the settling tank of oily sewage treating device using EC. The 1st and 3rd baffles flowing in from the inlet have lower gaps. The 2nd and 4th baffles have upper gaps. The lower clearance was set to A and the upper clearance to B. To investigate the influence of baffle clearance on the flow fluid distribution in the settling tank thoroughly, 5 sets of equal upper and lower gaps and 13 sets of unequal upper and lower gaps were simulated.

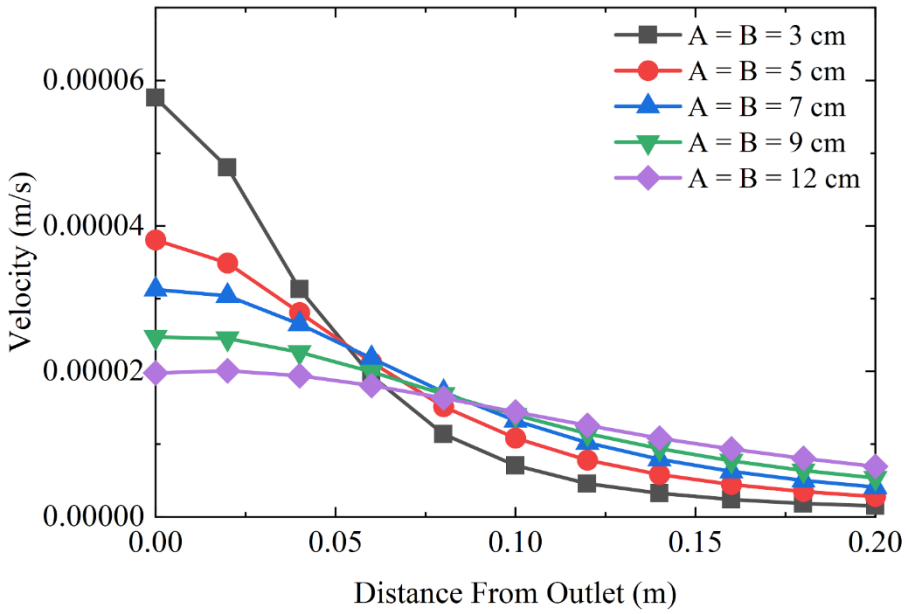

Figure 6. Velocity distribution along the horizontal direction at the outlet of the baffle with different clearances

When the gaps between the upper and lower baffles were the same, the velocities at each gap would not significantly different. And the fluid flows at a uniform speed between the baffles. Although no violent collision would cause flocs to break, it may also affect the growth of particles due to mixing. After the fluid passed through the 4th baffle, a jet with a higher velocity will appear, which will be strongly mixed with the surroundings. The degree of mixing is related to the baffle clearance. The smaller the gap, the greater the velocity of flow through the gap and the stronger the mixing with the surroundings. When the gap was 3 cm, the jet speed at the outlet was the highest. The attenuation speed was also the fastest. And the attenuated speed was lower than that of other sets. It might cause severe collision due to the excessive velocity of the jet at the initial stage, which leads to the breakage of the flocs. At the same time, excessive attenuation rate of jet velocity at later stage results in insufficient mixing effect. As the gap increased, the velocity attenuation curve at the baffle outlet became smoother. The exit velocity decreased and the velocity after attenuation increases gradually. The disadvantage to floc growth caused by a small gap is avoided.

It can be seen from Figure 7(a) that when the baffle gap was 3 cm, multiple velocity gradients could be observed. But the difference between them was not obvious. When the baffle gap was increased to 7 cm, each velocity gradient area could be distinguished. The number of velocity gradients did not decrease immediately while the gap increases to 9 cm. However, as the clearance continues to increase, the velocity gradients tend to merge. To make EC particles grow well at the initial stage and have a strong mixing effect at the later stage, the flow field with baffle clearance of 7 cm and 9 cm was considered to be better by comparison.

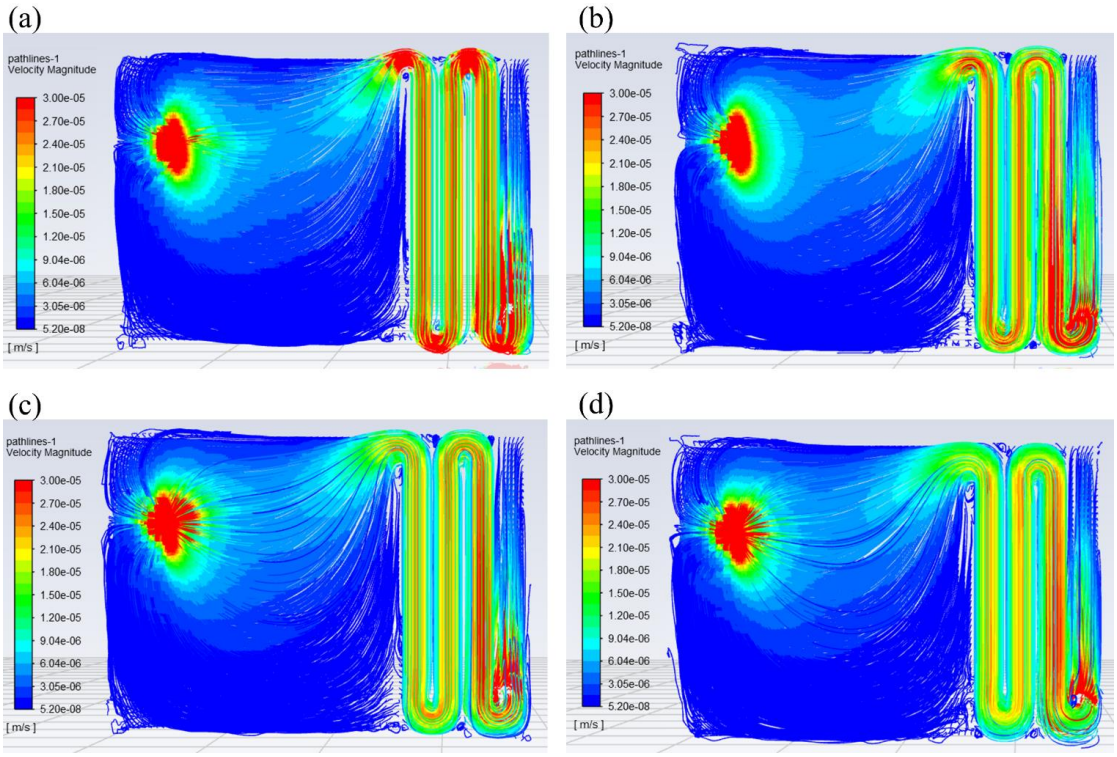

Figure 7. Streamline of sedimentation tank with different clearances: (a) A = B = 3 cm, (b) A = B = 7 cm, (c) A = B = 9 cm, (d) A = B = 12 cm

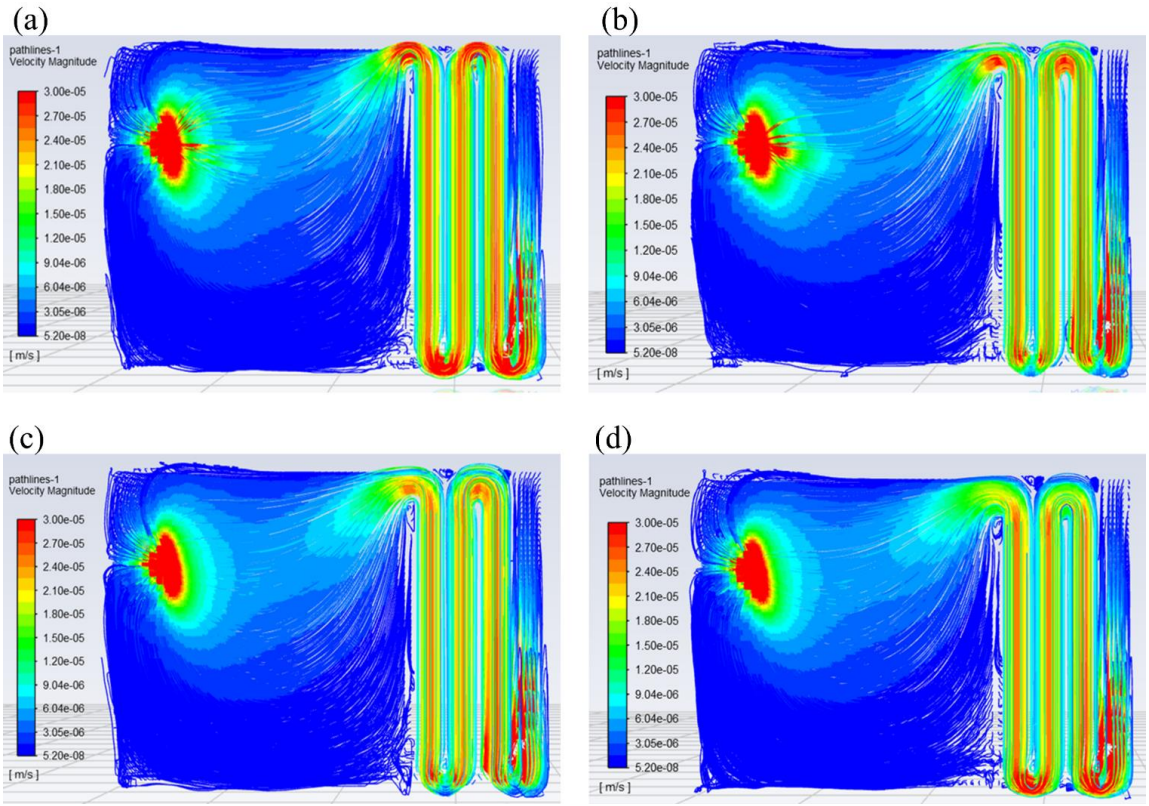

Figure 8. Streamline diagram of sedimentation tank with different upper and lower clearances: (a) A = 3 cm, B = 5 cm, (b) A = 3 cm, B = 7 cm, (c) A = 3 cm, B = 9 cm, (d) A = 3 cm, B = 12 cm

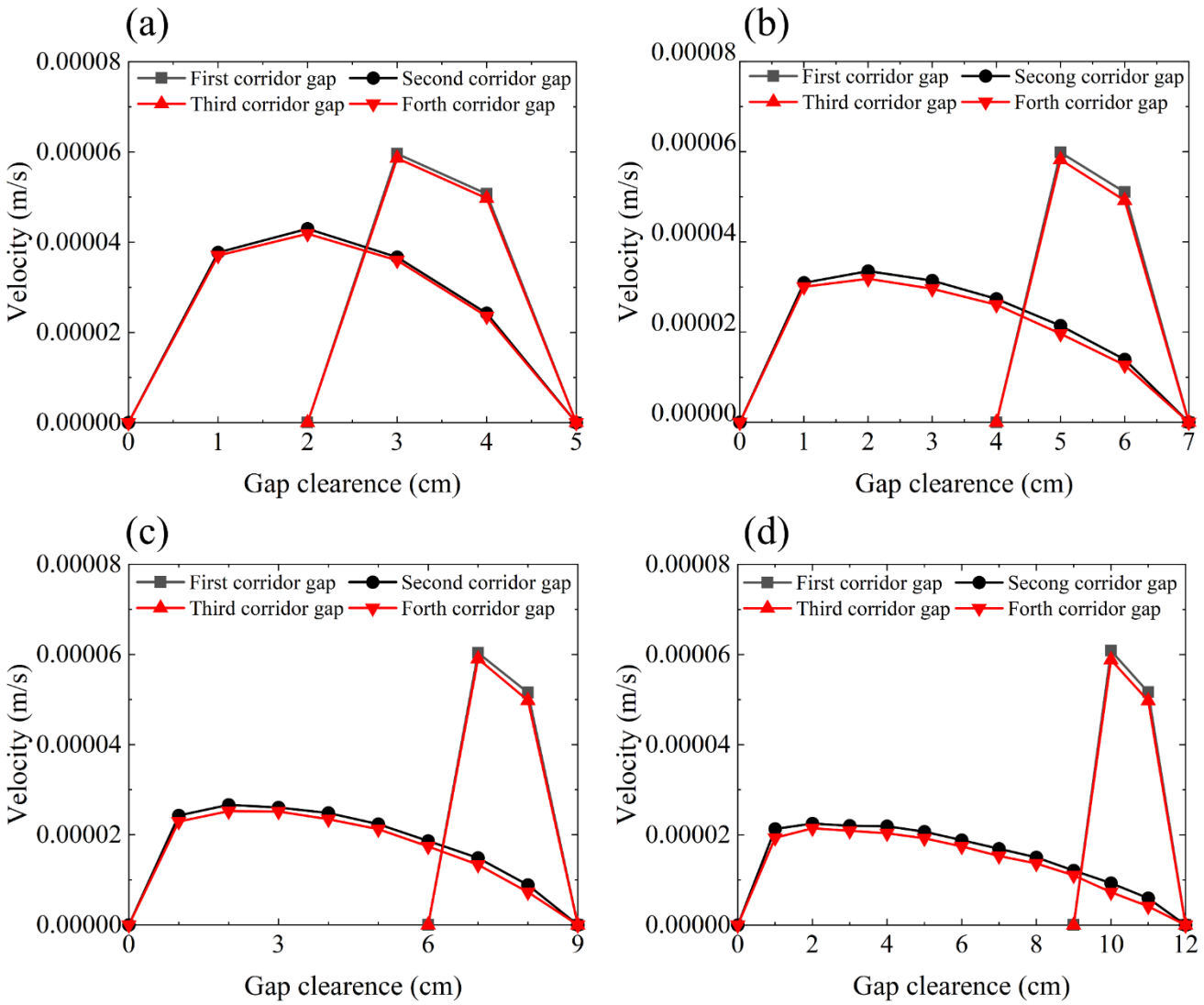

Figure 9. Velocity comparison diagram with different upper and lower clearances: (a) A = 3 cm, B = 5 cm, (b) A = 3 cm, B = 7 cm, (c) A = 3 cm, B = 9 cm, (d) A = 3 cm, B = 12 cm

When the upper and lower baffle clearances were different, the effect of changing the baffle clearance on the fluid distribution at the outlet was the same as that of when the upper and lower baffle clearances are equal. As shown in Figure 8 and Figure 9, the clearance between the upper and lower baffles has a great influence on the velocity at the gap. The larger the gap difference, the larger the speed difference at the gap. In the presence of velocity difference, high-speed fluid can impact low-velocity fluid to form mixing effect, which is beneficial to the growth of EC particles. However, when the speed difference was large, the impact of high-speed fluid on low-speed fluid was excessive, which would lead to floc breakage. In the initial stage of EC, the particles are small, and a higher flow rate is required to increase the collision probability of the particles and enhance the mass transfer. After the flocs become larger in the later stage, the shear resistance of particles decreases and a lower flow rate is needed. When choosing the baffle gap in practice, the speed difference and the growth condition of particles should be considered comprehensively, and the gap should be selected reasonably to meet the growth conditions

of flocs.

4. EXPERIMENT AND OPTIMIZATION OF SEDIMENTATION TANK

4.1 Experiments and data analysis

Based on the previous flow field simulation, the design parameters of the sedimentation tank were obtained. And the equipment processing and oil-bearing sewage purification performance test were carried out. The experimental steps are as follows:

(1) Water, edible oil, and edible salt were used to prepare oily sewage for the experiment, and fill the sewage into the oily sewage treatment device.

(2) Open the EC reactor to remove the gas from the unit.

(3) Turn on the power supply with a constant current of 15 A.

(4) Open the air pump in the air floating area, and open the intake pump in the water storage tank and the suction pump between storage tank and reactor respectively to regulate the sewage flow.

(5) Samples were taken at the outlet of the storage tank and sedimentation tank at intervals of 30 minutes, and the oil content and turbidity of the sample were tested. The entire experimental process was 150 minutes.

The experimental data were as follows:

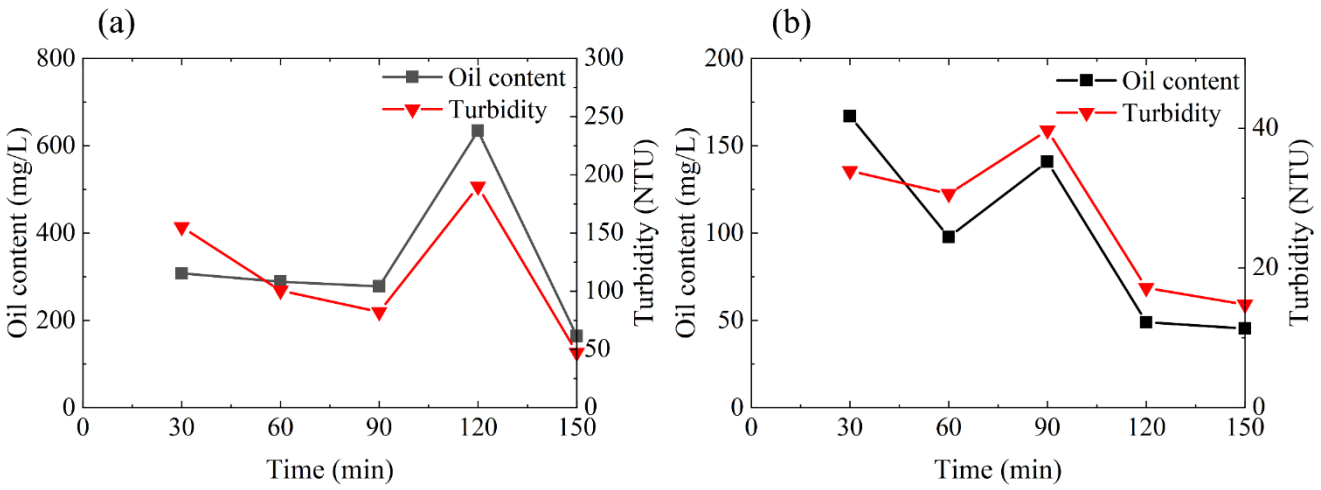

Figure 10. Curve diagram of oil content and turbidity in (a) storage tank and (b) sedimentation tank

As can be seen from Figure 10, the concentration and turbidity of the outlet of storage tank and sedimentation tank decreased with time as a whole. Moreover, a bulge could be seen in the curves of Figure 10. The reason for the bulge in Figure 10(a) was the existence of the overflow pipe. When the water level of the sedimentation tank reached the height of the overflow pipe, the fluid in the sedimentation tank would flow back to the water storage tank. Reflux fluid carries some flocs. During the reflux process, the oil droplets were desorbed under the action of shearing, resulting in a brief

recovery of the oil content in the storage tank. The reason for the bulge in Figure 10(b) was that a large number of flocs accumulated on the surface of the sedimentation area after the reaction for a while. Part of flocs with loose structures were sheared into small particles by the flow in the sedimentation area, resulting in the rise of turbidity. Meanwhile, under the action of shear force, the oil droplets attached to the floc surface were desorbed, causing a temporary increase of oil content in the sedimentation tank. By calculating the concentration and turbidity at the beginning and the end, the turbidity and oil removal rates after 150 minutes were 90.49% and 85.27% respectively.

In summary, the treatment process would be subject to fluctuations in the presence of overflow fluid in the sedimentation tank. The integrated EC oily sewage treatment device still had room for optimization. The structural parameters of the sedimentation tank would continue to be optimized.

4.2 Flow field simulation and optimization of sedimentation tank

This optimization aims to improve the flow field distribution of the sedimentation tank by changing the position of the upper and lower clearance of the baffle, the ratio of the baffle clearance to the corridor width, and the corridor width.

4.2.1 Changing the position of the upper and lower clearance of the baffle

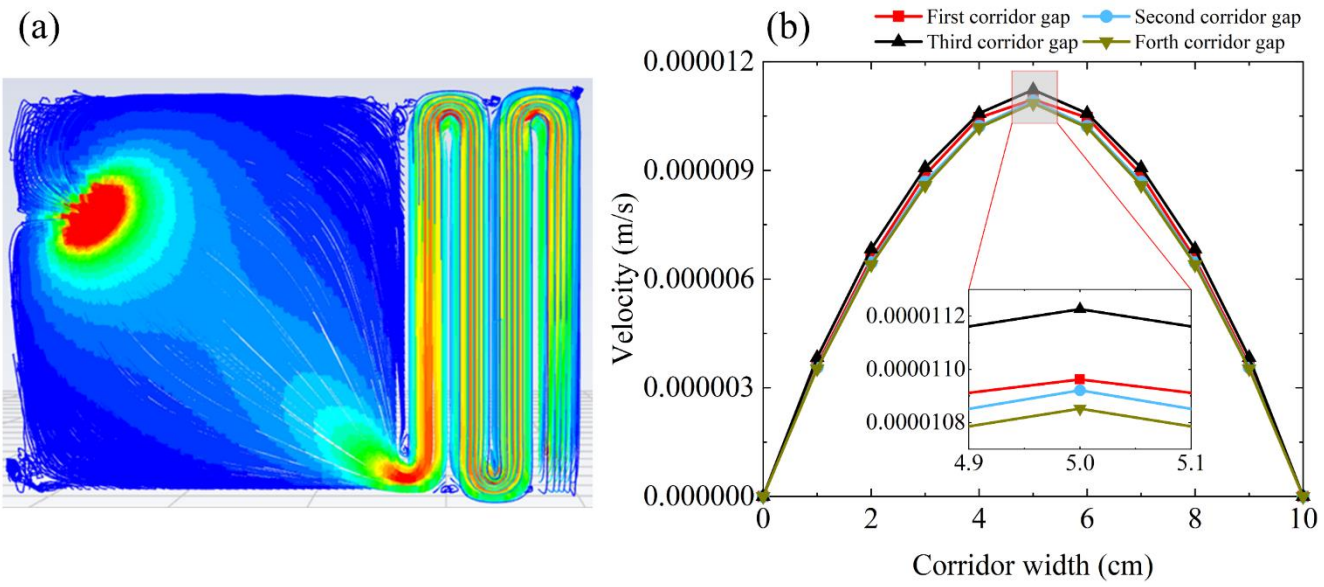

Figure 11. Velocity distribution in sedimentation tank after changing the position of the upper and lower clearance of the baffle: (a) Streamline diagram, (b) Speed in corridor

As can be seen from Figure 8, since the inlet of the sedimentation tank is on the downside side, the upper area of the first gallery entering the settling tank is close to the dead zone. Through the analysis in section 3.2, it was found that when the upper and lower baffle gaps were the same and the gap was 7 cm, the flow field distribution was better. Consequently, this optimization would mirror the four baffle positions up and down based on the gap of 7 cm. After mirroring, the 1st and 3rd baffles circulate on the

upper side, and the 2nd and 4th baffles circulate on the lower side. By contrast between Figure 8 and Figure 11, the dead zone that originally existed on the side of the first gallery disappeared. And the velocity distribution among the four corridors was relatively uniform. However, as can be seen from Figure 11, the speed difference at the centerline of each corridor is very small, resulting in an insufficient collision of particles. And failure to content the velocity environment for particles at the initial stage of the reaction.

4.2.2 Changing the ratio of the baffle clearance to the corridor width

Zhang[34] have found that the ratio of gap clearance to corridor width at the bend of baffle has a certain influence on the flow field. Set gap clearance at corners to L_1, and corridor width to L_2. And $L=L_1/L_2$. The influence of L to flow field distribution was explored when it was 0.7, 1, and 1.4. Through section 3.2 and 4.2.1, it was found that when the upper and lower gaps of the baffles were the same, the speed difference at each gap and the centerline of each corridor is not much different. Therefore, only the velocities at the second gap and the center of the third corridor were selected and sorted into Figure 12.

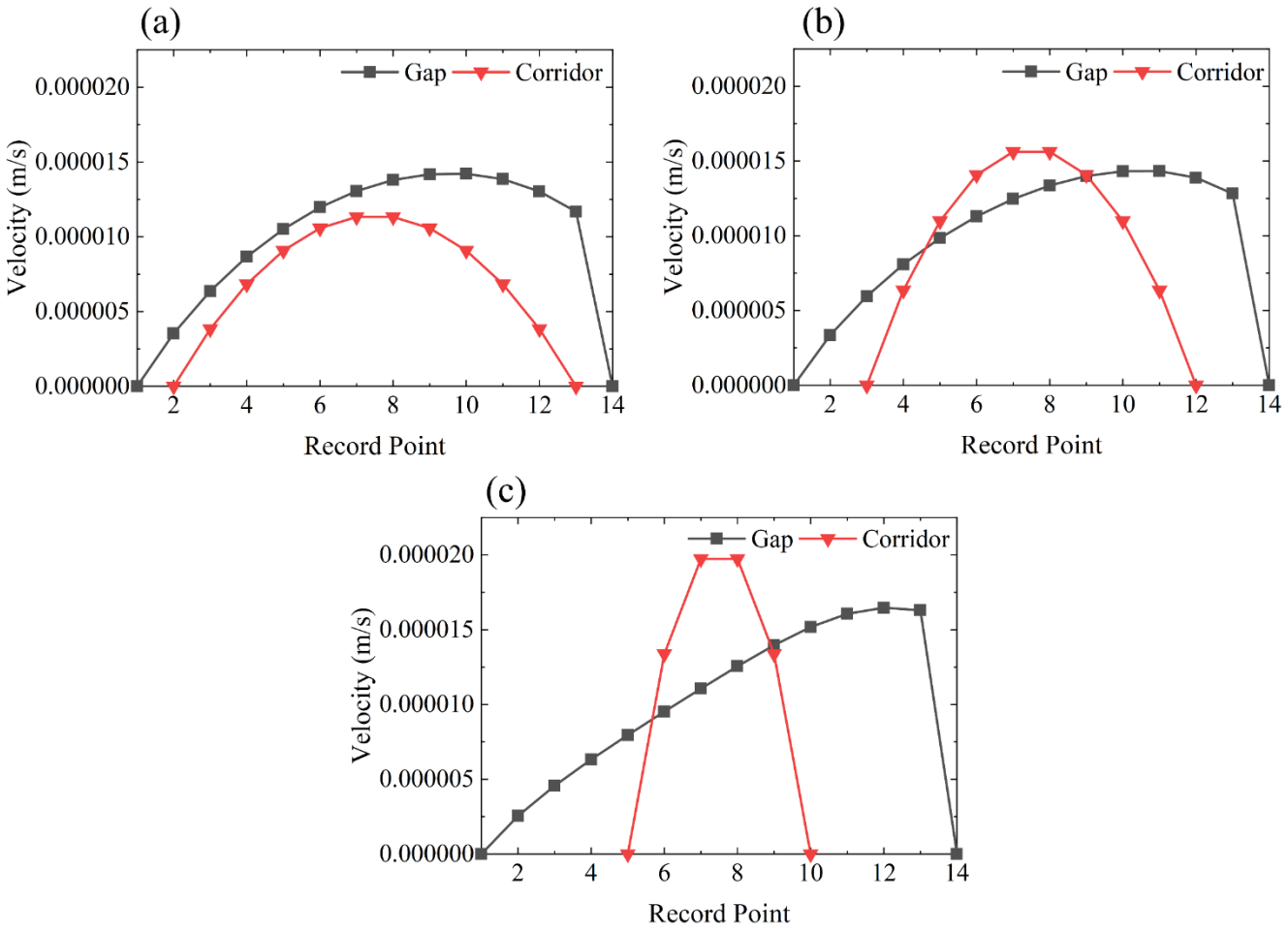

Figure 12. Velocity distribution at gallery and gap with different ratio of the baffle clearance to the corridor width: (a) L = 0.7, (b) L = 1, (c) L = 1.4

As the original device structure which L= 0.7, the speed at the corner was greater than that of the corridor. The high-speed flow from the corner might have a large shear effect on the particles, which was easy to cause the breakage of the flocs. When L = 1.4, the overall speed at the corner is lower. And the maximum speed is less than that of the corridor. Therefore, it cannot be mixed well with gallery fluid. It is also possible that the floc would not be removed because the speed is too low to take away the flocs at the corner so that the floc precipitates prematurely at the sedimentation tank. While L = 1, the speed at the corner is moderate. It would neither cause floc breakage due to too high speed, nor a low mixing effect and premature floc settling due to too low speed. It is the best parameter for the ratio of baffle clearance to corridor width.

4.2.3 Changing the corridor width

Considering the flocs have different requirements for fluid velocity in different periods, the flow velocity in the baffle area would be designed differently. At the initial stage of EC, the particles are small, and a larger flow rate is required to increase the collision probability between the particles. After the flocs become larger in the later stage, the shear resistance capacity decreases, and a lower flow rate is required to avoid breaking. According to the analysis in section 3.2, the flow field was better when the baffle clearance was 7 cm and 9 cm, so the clearance of 7cm and 9cm was selected for this optimization. The baffle clearance and gallery width of the first two baffles were set to 7 cm and the last two were set to 9 cm. And continue the optimum design of 4.2.1 and 4.2.2.

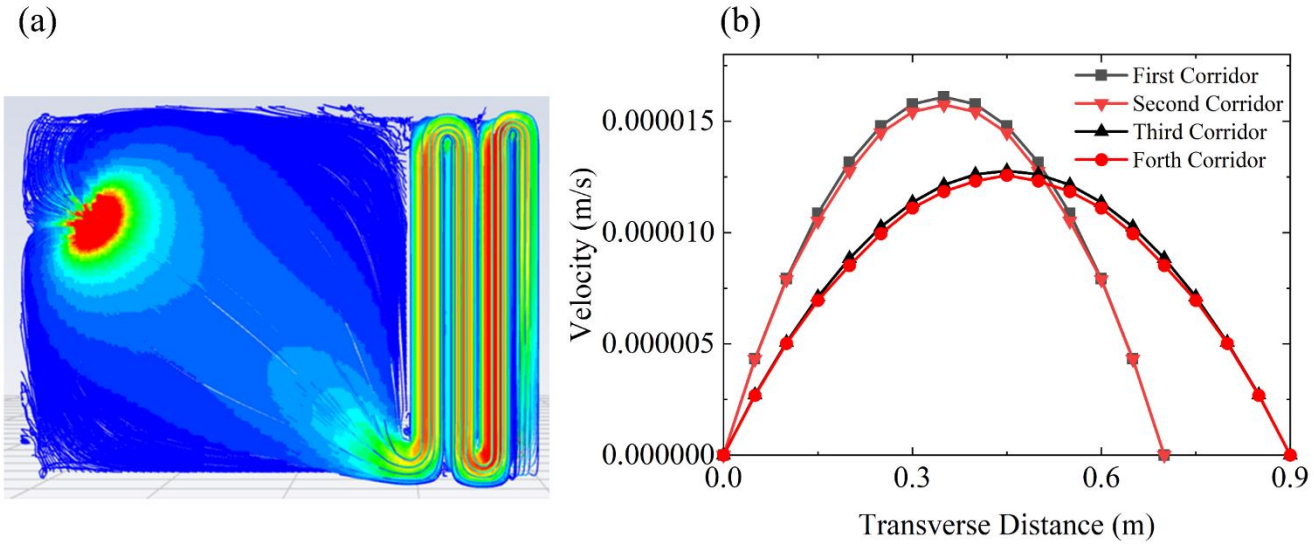

Figure 13. Velocity Distribution in Corridor after Changing the corridor width: (a) Streamline diagram, (b) Speed in corridor

The optimized flow field effect has been relatively ideal, which can meet the speed requirements of flocs in different periods[35]. At the first two baffles, the corridor width was narrow and the flow velocity was large, which could enhance mass transfer. At the latter two baffles, the gallery become wider and the fluid velocity became slower. Under the better effect of mass transfer brought by high-

speed flow at the early stage, the flocs formed large, and the shear resistance of the flocs decreases. Lower speed just prevents the floc from breaking up. Therefore, the baffle structure was set from narrow to wide, which provided a better speed environment for floc growth during settling process and helped to improve the treatment efficiency of integrated EC device.

5. CONCLUSION

(1) The fluid would form a jet after passing through the baffle. When the flow rate was small, the jet decayed rapidly and could not mix well with the surroundings. When the flow rate was large, a large disturbance would be generated, and the mixing would be enhanced. However, it might produce a strong impact force and result in floc breakage. The multi-velocity gradient created a suitable environment for efficient collision of particles and growth of floc, which is more conducive to the formation of larger flocs and higher density. The number of velocity gradients also increases as the flow increases from 0.5 $m^3 h^{-1}$. When 2 $m^3 h^{-1}$ was reached, the number of velocity gradients did not change. After continuing to increase the flow rate, the velocity gradient had a trend to decrease.

(2) The clearance of the baffle in the sedimentation tank can also affect the flow field distribution. When the gaps were 3 cm and 5 cm, due to the small flow area at the gap, the water flow would generate a large pressure. The fluid flowing through the gap would generate a large velocity, which had a strong impact on the subsequent fluid causing floc breakage. While the gap was 12 cm, the fluid flow through the gap was slow. It could not mix well with the surrounding fluid at the initial stage, resulting in the growth of flocs negatively.

(3) Experiments were carried out with designed integrated oily sewage treatment device and it was found that turbidity and concentration generally decreased with increasing reaction time. Overflow pipe in sedimentation tank would affect the purification process. The turbidity and oil removal rates were 90.49% and 85.27% respectively. The results show that there is still some optimization space for this device.

(4) According to the previous flow field simulation and experiment, it was found that the structure of the sedimentation tank has a great impact on the treatment efficiency of the integrated device. Therefore, the settlement tank would be optimized by changing the position of the upper and lower clearance of the baffle, the ratio of the baffle clearance to the corridor width, and the corridor width. Finally, the position of the baffle was mirrored up and down, the ratio between the baffle gap and the corridor width was set to 1, the width of the first two corridors was set to 7 cm, and the width of the last two corridors was set to 9 cm. At this time, the flow field distribution in the device is ideal, which conforms to the growth law of flocs.

ACKNOWLEDGMENTS
This work was supported by the National Natural Science Foundation of China (Grant No. 51904326), Natural Science Foundation of Shandong Province (Grant No. ZR2019MEE105 and ZR2019MEE011), the Science and Technology Plan Projects of Qing Dao (19-6-1-87-nsh), and Open Research Fund Program of Shandong Provincial Key Laboratory of Oilfield Produced Water Treatment and

Environmental Pollution Control (Sinopec Petroleum Engineering Corporation, No.10205363-21-ZC0607-0004, No. 10205363-21-ZC0607-0006).

References

1. M.A. Cohen, *Encyclopedia of Energy, Natural Resource, and Environmental Economics*, (2013) 121
2. I. Radelyuk, K. Tussupova, J.J. Klemeš, and K.M. Persson, *J. Cleaner Prod.*, 302 (2021) 126987
3. J.X. Loi, A.S.M. Chua, M.F. Rabuni, C.K. Tan, S.H. Lai, Y. Takemura, and K. Syutsubo, *Sci. Total Environ.*, 832 (2022) 155067
4. A. Ullah, H.J. Tanudjaja, M. Ouda, S.W. Hasan, and J.W. Chew, *J. Water Process Eng.*, 43 (2021) 102293
5. C. Zhao, J. Zhou, Y. Yan, L. Yang, G. Xing, H. Li, P. Wu, M. Wang, and H. Zheng, *Sci. Total Environ.*, 765 (2021) 142795
6. F. Sher, A. Malik, and H. Liu, *J. Environ. Chem. Eng.*, 1 (2013) 684
7. F. Ding and M. Gao, *Adv. Colloid Interface Sci.*, 289 (2021) 102377
8. G.Z. Kyzas and K.A. Matis, *J. Mol. Liq.*, 220 (2016) 657
9. A.-M.G. Harik, Z. Griffiths, and T.C. Hazen, *Curr. Opin. Chem. Eng.*, 36 (2022) 100800
10. K. Padmaja, J. Cherukuri, and M. Anji Reddy, *J. Water Process Eng.*, 34 (2020) 101153
11. T.K. Hussein and N.A. Jasim, *Mater. Today:. Proc.*, 42 (2021) 1946
12. P.P. Das, M. Sharma, and M.K. Purkait, *Sep. Purif. Technol.*, 292 (2022) 121058
13. Y.-m. Chen, W.-m. Jiang, Y. Liu, and Y. Kang, *Chemosphere*, 250 (2020) 126128
14. L. Szpyrkowicz, *Industrial & Engineering Chemistry Research*, 44 (2005) 7844
15. M.A. Sadik, *Advances in Chemical Engineering and Science*, 09 (2019) 182
16. A. Shokri and M.S. Fard, *Chemosphere*, 288 (2022) 132355
17. P.K. Holt, G.W. Barton, and C.A. Mitchell, *Chemosphere*, 59 (2005) 355
18. Y. Liu, Y. Chen, W. Jiang, and T. Wang, *J. Electrochem. Soc.*, 166 (2019) E533
19. Y. Liu, X. Zhang, W. Jiang, M. Wu, and Z. Li, *Chem. Eng. J.*, 417 (2021) 129310
20. W.-m. Jiang, Y.-m. Chen, M.-c. Chen, X.-l. Liu, Y. Liu, T. Wang, and J. Yang, *Sep. Purif. Technol.*, 211 (2019) 259
21. P.N. Alam, Yulianis, H.L. Pasya, R. Aditya, I.N. Aslam, and K. Pontas, *Mater. Today:. Proc.*, (2022)
22. N.A. Rahman, C.J. Jol, A.A. Linus, F.L. Dampam, N.S.A. Jalal, N. Baharudin, and W.W.S.W. Borhan, *Chemical Engineering and Processing - Process Intensification*, (2022) 108967
23. R. Zhang, Y. Xu, L. Shen, R. Li, and H. Lin, *J. Membr. Sci.*, 653 (2022) 120541
24. F. Özyonar and M.U. Korkmaz, *Chemosphere*, 290 (2022) 133172
25. W. Jiang, M. Chen, J. Yang, Z. Deng, Y. Liu, J. Bian, S. Du, and D. Hou, *J. Electroanal. Chem.*, 801 (2017) 14
26. X.J Wang, Beijing University of Chemical Technology, (2019)
27. Z.H. Di, L. Zhou, Y. Bai, K.K. Ma, Z. Cao, and H.Z. Zhang, Water & Wastewater Engineering, 56 (2020) 513
28. S. Martinez-Delgadillo, H. Mollinedo-Ponce, V. Mendoza-Escamilla, C. Gutiérrez-Torres, J. Jiménez-Bernal, and C. Barrera-Diaz, *J. Cleaner Prod.*, 34 (2012) 120
29. T. Höhne, V.F. Asl, L. Ople Villacorte, M. Herskind, M. Momeni, D. Al-Fayyad, S. Taș-Köhler, and A. Lerch, *Water*, 13 (2021)
30. P. Song, Q. Song, Z. Yang, G. Zeng, H. Xu, X. Li, and W. Xiong, *J. Environ. Manage.*, 228 (2018) 336
31. J. Bridgeman, B. Jefferson, and S. Parsons, *Chem. Eng. Res. Des.*, 86 (2008) 941
32. Y. Yuan and R.R. Farnood, *Powder Technol.*, 199 (2010) 111
33. D.D. Zhou, W.Y. Zhao, J. Wang, C.X. Tan, S.S. Dong, and N. Cui, Journal of Jilin University

(Earth Science Edition), 42 (2012) 1896
34. H.L. Zhang, Y.B. Wu, and F.Y. Cui, Journal of Shenyang Architecture University (Natural Science Edition), (2006) 981
35. *Enr Engineering News Record*, (2007)